

RESEARCH ARTICLE

10.1002/2015JC010808

A comparison of methods for estimating directional spectra of surface waves

M. Donelan¹, A. Babanin², E. Sanina², and D. Chalikov²¹Department of Ocean Sciences, Rosenstiel School of Marine and Atmospheric Science, University of Miami, Miami, Florida, USA, ²Centre for Ocean Engineering, Science and Technology, Swinburne University, Melbourne, Victoria, Australia

Key Points:

- Comparison of the three main methods of estimating directional wave spectra
- Wind waves are examined
- Computer-generated waves of known spreading are tested

Correspondence to:

M. Donelan,
mdonelan@rsmas.miami.edu

Citation:

Donelan, M., A. Babanin, E. Sanina, and D. Chalikov (2015), A comparison of methods for estimating directional spectra of surface waves, *J. Geophys. Res. Oceans*, 120, doi:10.1002/2015JC010808.

Received 3 MAR 2015

Accepted 21 JUN 2015

Accepted article online 24 JUN 2015

Abstract Three methods of estimating the directional spectra of water waves are intercompared. The Maximum Likelihood Method (MLM) and the Maximum Entropy Method (MEM) require stationarity of the time series and yield only the frequency-direction spectra. The Wavelet Directional Method (WDM) does not require stationarity and also yields the wave number-direction spectra and is suitable for event analysis. The comparison includes three cases of wind-generated waves on a large lake and two cases of model-generated waves with different directional spreading. The comparisons of the frequency-direction spectra show that the Wavelet Directional Method yields the best estimates of the directional spectra.

1. Introduction

In situ wave directional information is usually gleaned from measurements of wave properties (e.g., surface elevation and slope vector) at a point or the same property (e.g., surface elevation) at three or more points. The directional analysis of surface waves generally starts from the assumption of stationarity of time series of wave properties. While a new conceptual basis for measurements of three-dimensional surface waves is emerging [e.g., Liu, 2013], spectral mapping of two-dimensional wavy surfaces remain the main means of such analysis. The methods in common use are: Maximum Likelihood Method (MLM) [Capon, 1979], Maximum Entropy Method (MEM) [Lygre and Krogstad, 1986], and Wavelet Directional Method (WDM) [Donelan et al., 1996; Krogstad et al., 2006]. These three methods do not yield the same directional spreads or even the same mean direction at each frequency. We compare the spreads via the ratio of downwave to cross-wave slopes from the time series and examine the mean direction variations with frequency.

The first two methods (MLM and MEM) are statistical and require (approximate) stationarity of the data (time series). They yield spectra that are consistent with the correlation matrix of the observations. The third method (WDM) estimates wavenumber, direction, and amplitude at each point in time; stationarity is not required. The resulting spectra are composed from the squares of the amplitudes of each wave observed, having frequency, wave number, direction, and amplitude. Both frequency-direction and wave number-direction spectra are obtained. The Wavelet Directional Method, therefore, may be applied to stationary processes as well as to such time variable phenomena as wave growth, decay or turning, tsunamis, acoustic, or seismic wave packets. It reports the waves that actually occurred during the time of data collection rather than the likelihood of waves occurring based on the statistics of correlations and cross correlations.

Intercomparison of the methods is first realized via surface elevation time series of wind-generated waves from Lake Ontario [Donelan et al., 1996]. Then we used the model of Chalikov and Babanin [2013] to generate an evolving surface on a dense grid. The model calculations are carried out on the wave number spectra and these are transformed to yield surface elevation time series at selected grid points $\{V_m(t) = \eta(x_m, y_m, t)\}_{m=1}^M$. The model wave number spectra provide a standard with which to assess the three methods that are based on the analysis of time series.

2. The Methods—MLM, MEM, and WDM

The starting point is a set of M measured time series $\{V_m(t) = \eta(x_m, y_m, t)\}_{m=1}^M$ of sensor readings in vector positions $\{\mathbf{r}_m\}$, $1 \leq m \leq M$ of some of the surface elevations. It is assumed that the series are recorded with

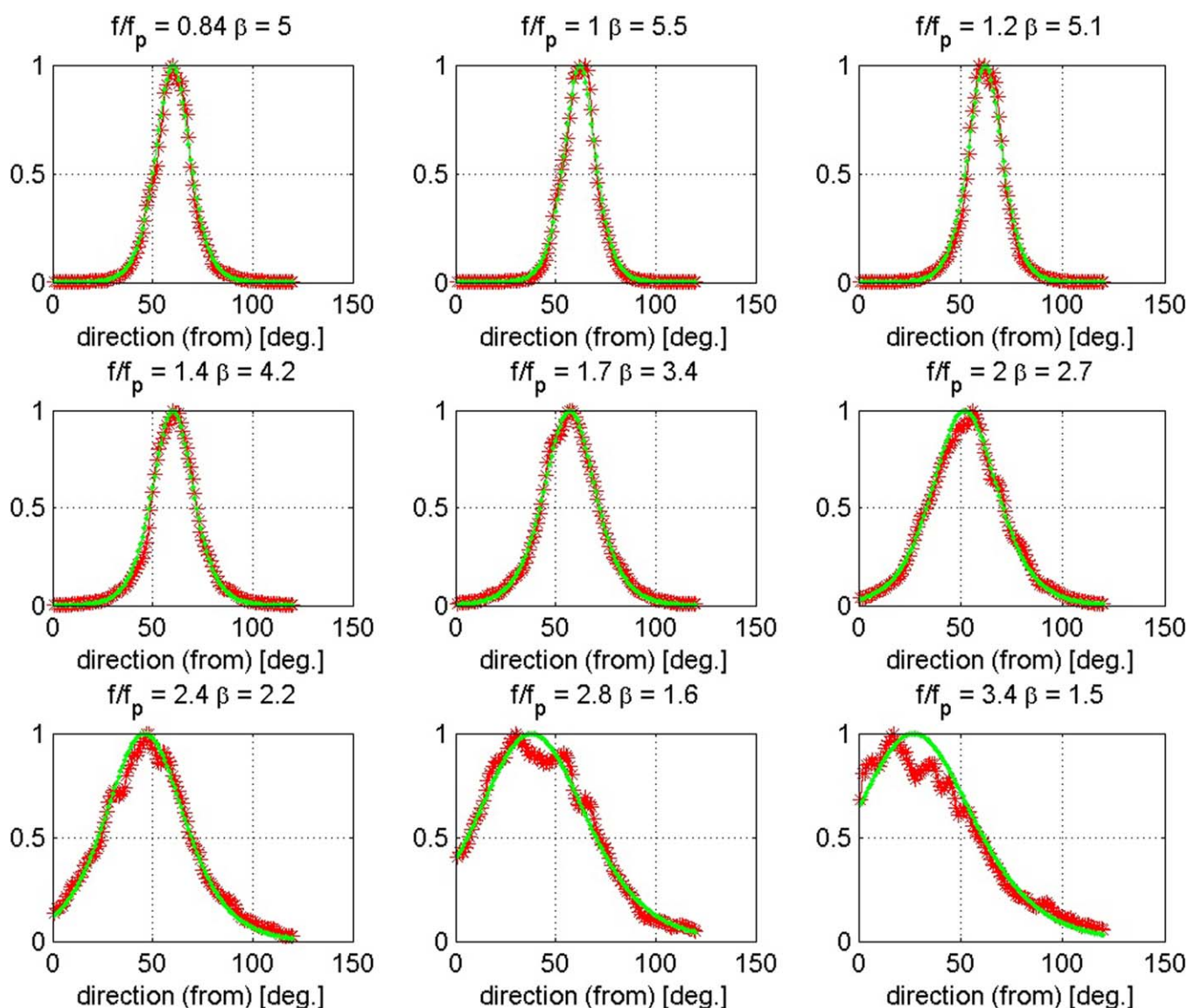


Figure 1. The spreading function at increasing frequencies for a case of light winds and long fetch—run 62. Observed spreading via WDM (red); fitted $\text{sech}^2(\beta(\theta - \theta_0))$ (green).

a certain sampling frequency ω_s , with N samples in each series over the time interval $0 \leq t \leq T$, where $T = 2\pi N / \omega_s$. The recording interval T will typically be rather long compared to the correlation time of the series [Krogstad, 1988]. We aim to obtain wave number-frequency spectrum estimate $\hat{S}(\mathbf{k}, \omega)$ of the field, where $\mathbf{k} = (k_x, k_y)$.

2.1. Maximum Likelihood Method

Capon [1969] developed a high-resolution method for seismic processing that later has become known as the Maximum Likelihood Method (MLM) for directional spectra. The method was introduced in the context of ocean wave spectra by Davis and Regier [1977] and Borgman [1985].

The motivation of the MLM procedure, given by Capon [1969], is based on the idea of constructing a linear space-time operator that when applied to a segment of the array data yields a minimum-variance unbiased linear estimate for the complex amplitude of a discrete plane wave with a particular wave number k_0 . If the spectral density matrix for the “noise” (components of the random field corresponding to wave numbers

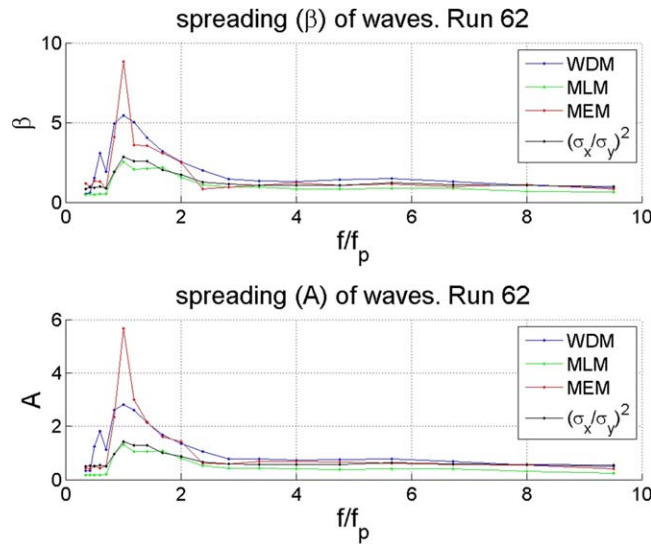


Figure 2. Spreading parameters for run 62 from the three methods and the ratio of downslope to cross slope.

other than k_0) was available, then the optimum amplitude estimator could be constructed. However, since there is no prior knowledge concerning the noise, an estimate for the total spectral density matrix (including both the signal and the noise) is used. The resulting operator is applied to separate, uncorrelated segments of the data, and the magnitudes of the complex amplitude estimates are squared and averaged together to give an estimate for the average plane wave power (that is, the variance of the plane wave complex amplitude) at wave number k_0 :

$$\hat{S}(\mathbf{k}, \omega) = [\zeta'(\mathbf{k})\chi_n^{-1}\zeta(\mathbf{k})]^{-1}, \quad (1)$$

where

$$(\chi_n)_{ij} = \overline{X_i(n\Delta\omega)X_j(n\Delta\omega)}, \quad (2)$$

$$X_m(n\Delta\omega) = \zeta_m(\mathbf{k}, n\Delta\omega)S(\mathbf{k}, n\Delta\omega), \quad (3)$$

$$\zeta_m(\mathbf{k}, n\Delta\omega) = \exp(i\mathbf{k} \cdot \mathbf{r}_m), \quad (4)$$

$$\zeta(\mathbf{k}) \equiv \{\zeta_m(\mathbf{k}, n\Delta\omega)\}^T, \quad m=1, \dots, M, \quad (5)$$

and the prime indicates conjugate transpose.

The estimation procedure is repeated at different wave numbers to yield a plot of estimated power versus wave number, which with appropriate normalization can be interpreted as a spectral density estimate [Marzetta, 1983].

2.2. Maximum Entropy Method

The concept of Maximum Entropy spectrum estimation Method (MEM) for one-dimensional time series is equivalent to fitting an autoregressive model to the data commonly referred to as the Box-Jenkins approach [Krogstad, 1988].

We assume that a time span of data, which has an estimate of the cross spectrum between any two sensors, is available:

$$\hat{P}_{ij}(\omega) \equiv \hat{P}(q_i, q_j, \omega) \approx \int_{-\infty}^{\infty} C(q_i, q_j, \tau) \exp(-i\omega\tau) d\tau, \quad (6)$$

where the cross covariance is

$$C(q_i, q_j, \tau) = E \left[[\eta(q_i, t+\tau) - M_{q_i}] [\eta(q_j, t) - M_{q_j}] \right]. \quad (7)$$

Given the cross spectra $\hat{P}_{ij}(\omega)$, $i, j=1, \dots, K$, we then seek an estimator $\hat{S}(\mathbf{k}, \omega)$ of the spectrum using entropy ideas. The multivariate version of time-domain maximum-entropy spectral analysis (for K time series) has been worked out by Nuttall [1976]. We have N time samples at all of M space points having two corresponding coordinates. Thus we consider ζ to be the vector of the totality of all of these samples, of dimension NM^2 , each sample being a random variable. Some joint probability function $p(\zeta)$ can be

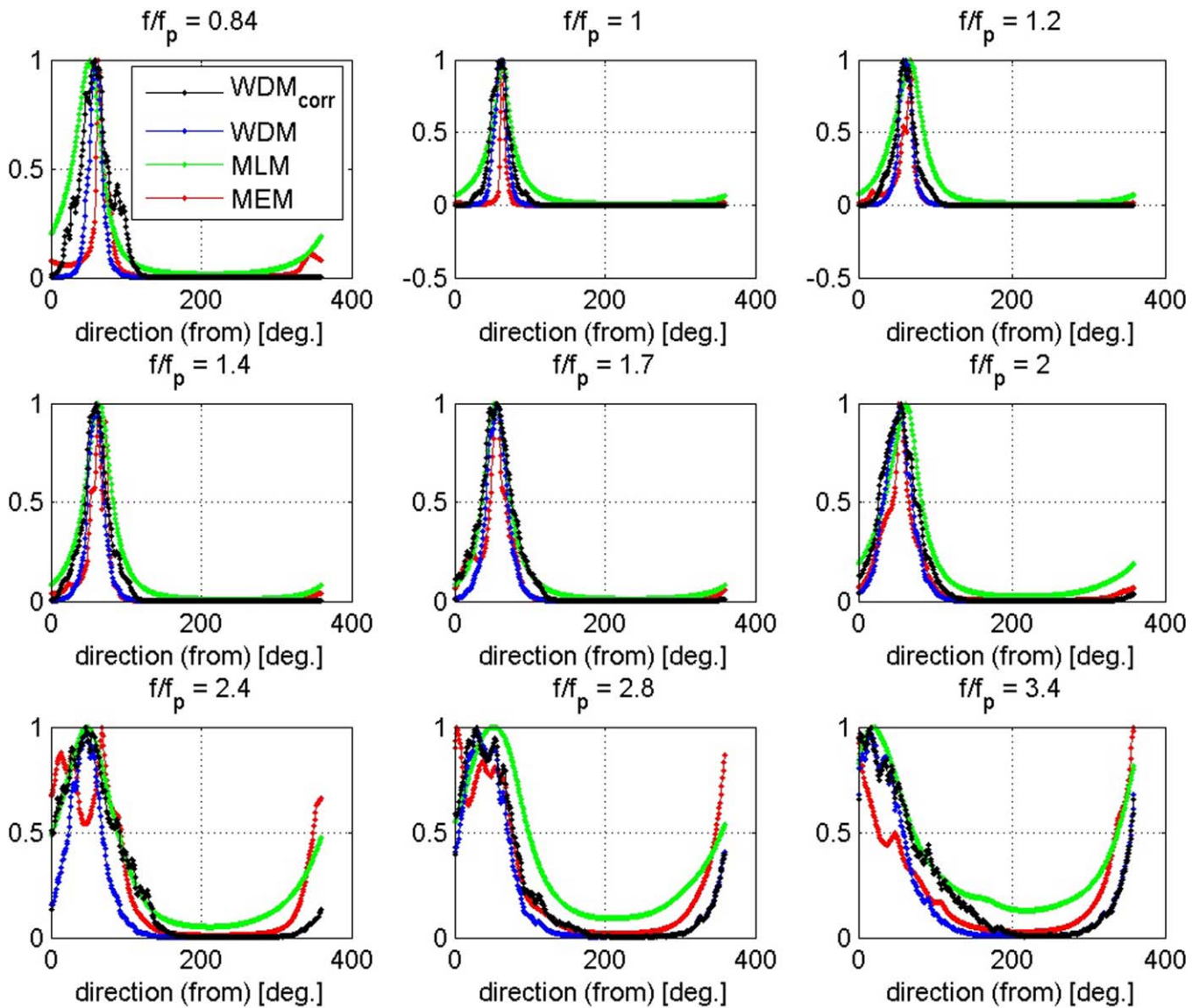


Figure 3. Comparative spreading for run 62 at various frequencies with respect to the peak.

considered. Assuming field $\eta(\mathbf{r}, t)$ to be Gaussian and maintaining band-limited assumptions, we obtain the entropy of the field.

We assume that the time-frequency processing is done separately and treat frequency as a fixed parameter. Thus we seek

$$\hat{S}(\mathbf{k}, \omega) = \max_{S(\mathbf{k}, \omega)} \int_1^M \int_1^M \ln S(\mathbf{k}, \omega) d\mathbf{k}. \quad (8)$$

The estimated cross spectrum is compatible with the estimated wave number spectrum

$$\hat{P}(\varrho_i, \varrho_j, \omega) = \int_R S(\mathbf{k}, \omega) \exp(i(\varrho_i - \varrho_j) \cdot \mathbf{k}) d\mathbf{k}, \quad i, j = 1, \dots, M. \quad (9)$$

The solution to the variational problem (8), (9)

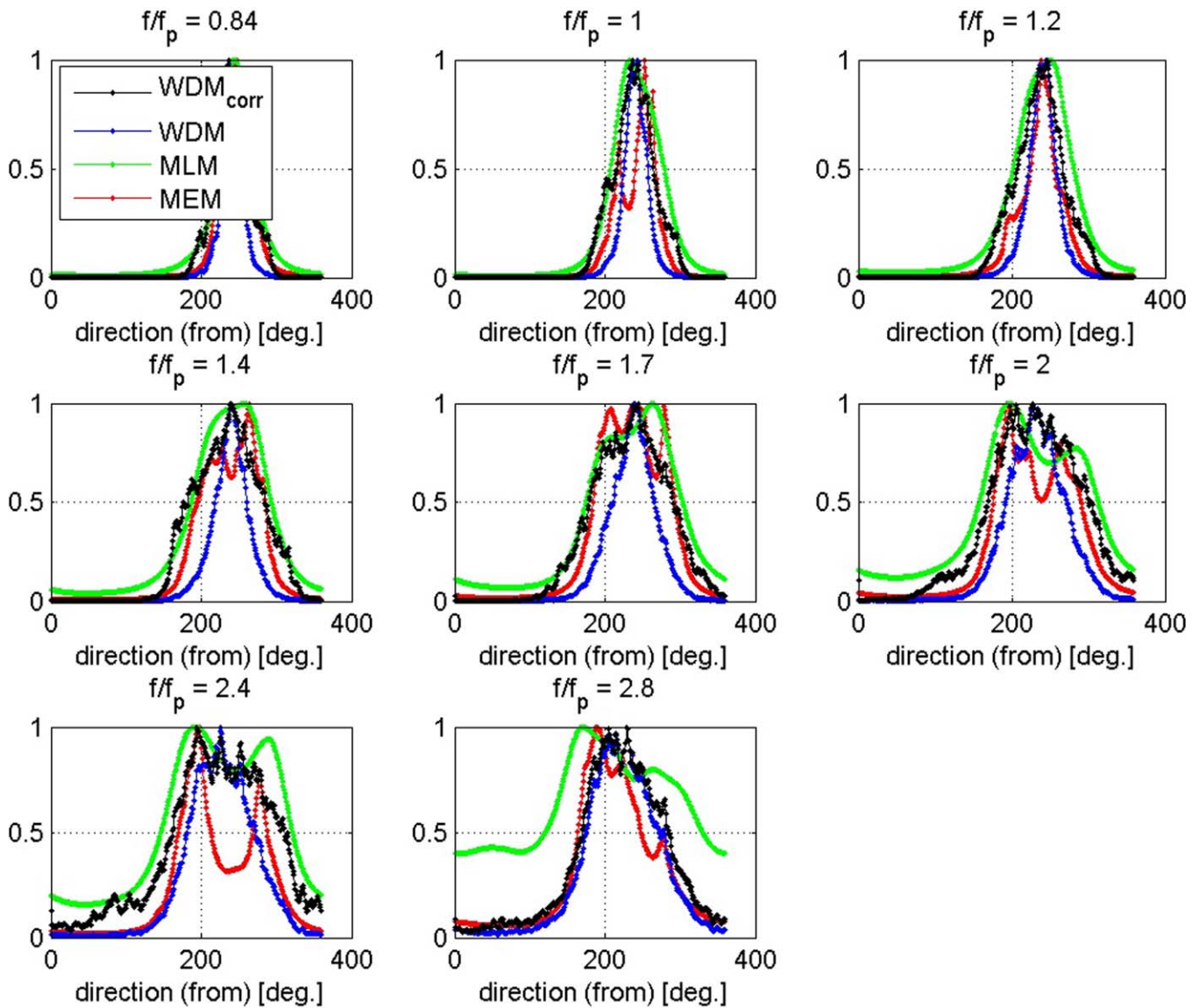


Figure 4. Comparative spreading for run 82 (short fetch, strong wind) at various frequencies with respect to the peak.

$$\widehat{S}(\mathbf{k}, \omega) = [\zeta'(\mathbf{k})\Lambda(\omega)\zeta(\mathbf{k})]^{-1}, \quad (10)$$

$$\int_R [\zeta'(\mathbf{k})\Lambda(\omega)\zeta(\mathbf{k})]\zeta(\mathbf{k})\zeta'(\mathbf{k})d\mathbf{k} = \widehat{P}(\omega), \quad (11)$$

where Λ is the matrix of the λ_{ij} , $\widehat{P}(\omega)$ is the estimated frequency cross-spectral matrix with elements $\widehat{P}_{ij}(\omega) = \widehat{P}(q_i, q_j, \omega)$ and the prime indicates conjugate transpose.

2.3. Wavelet Directional Method

Wavelet Directional Method (WDM) was introduced by Donelan *et al.* [1996]. WDM uses wavelet analysis techniques [see Farge, 1992; Kaiser, 1994]. For this purpose, Morlet wavelets are employed in our analysis. WDM differs from other methods in that the wave number and amplitude of each wave in each frequency band are identified at each sampling time step. WDM derives direction from phases of the wavelet transforms of the surface elevation data at three or more wave staffs. Thus the directional resolution depends on the precision of location of the staffs and is typically better than 1 degree. The resulting general directional wave number and frequency spectra are specified in terms of parameters, associated with spreading and wave development.

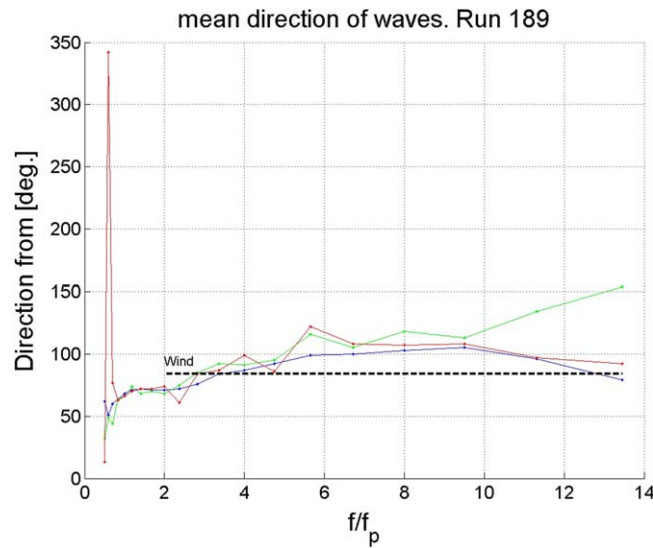


Figure 5. Mean directions for run 189 (long fetch, strong wind). WDM (blue), MLM (green), and MEM (red).

The Wavelet Directional Method (WDM) makes two assumptions: that the water surface can be represented by a sum of wavelets and that there is only one wave number in each frequency band at each time step. Considering the time series $\{\{V_m(t)\}\}_{m=1}^M$ of N records for all of the wave staffs, the first step is to obtain the (complex) wavelet transform of the M data sets at N discrete frequencies ω_q , $q=1, \dots, N$: W_{qp}^i , $i=1, \dots, M$. Thus for each chosen frequency ω_q we now have a time series of the amplitude and phase of that component. Pairs of the wave staffs (i and j) yield the measured phase differences ϕ_{ij}

$$\phi_{ij} = kr_{ij} \cos(\theta - \alpha_{ij}), \quad (12)$$

where (r_{ij}, α_{ij}) are the separation vectors of pairs of staffs, and $\mathbf{k} = (k, \theta)$ is the wave number vector at the chosen frequency and time.

It can be shown [Donelan et al., 1996] that the wave number vector may be determined from two pairs of staffs as

$$k = \left[\frac{\phi_{ab}}{r_{ab}} \sin \alpha_{cd} - \frac{\phi_{cd}}{r_{cd}} \sin \alpha_{ab} \right] / [\sin(\alpha_{cd} - \alpha_{ab}) \cos \theta], \quad (13)$$

$$\theta = \arctan [(\Gamma \cos \alpha_{cd} - \cos \alpha_{ab}) / (\sin \alpha_{ab} - \Gamma \sin \alpha_{cd})], \quad (14)$$

where $\Gamma = \frac{\phi_{ab}}{\phi_{cd}} \cdot \frac{r_{cd}}{r_{ab}}$ and the pairs ab and cd are chosen so that the angular difference between their separation vectors ($\alpha_{ab} - \alpha_{cd}$) is close to 90° or 270° . If there are more than two pairs (i.e., more than three wave staffs), multiple estimates of \mathbf{k} are obtained and the means and standard deviations of the estimates of \mathbf{k} may be calculated. Finally, the directional spectrum is calculated by distributing the energy ($|W_{qp}^i|^2$) at each time into the calculated wave number bins.

The summation runs over wavelets with different spatial extent and frequency, with no requirement for a unique dispersion relationship linking them. As a result, the wavelet approach is very flexible when considering nonhomogeneous data or data where the dispersion relationship between wave number and frequency is unknown.

3. Data Description

3.1. Field, Wind-Generated Waves

These data were obtained on the Lake Ontario tower of Canada's National Water Research Institute in 1987 [Donelan et al., 1996]. The tower is 1.1 km from the western shore and is exposed to fetches of 1.1 to 300 km. It was equipped with a six gauge (centered pentagon) array of capacitance wave staffs. Data were sampled at 4 Hz for at least an hour in each case.

3.2. Model, Computer-Generated Waves

An exact numerical scheme for the simulation of three-dimensional potential fully nonlinear periodic gravity waves [Chalikov and Babanin, 2013] is employed to produce surface elevations, $\eta(x, y, t)$, on a 1024×256 grid of area $4992 \text{ m} \times 4992 \text{ m}$. The input spectrum follows JONSWAP [Hasselmann et al., 1973] with the peak at 0.1 Hz and fixed spreading at all frequencies. Both wide spreading, $\cos^2 \theta$ and very narrow spreading, $\cos^{16} \theta$ were tested. The model was run for 60,000 time steps of 0.045 s. This corresponds to 270 peak periods or three-quarters of an hour—typical of field data. The waves evolve in the absence of wind.

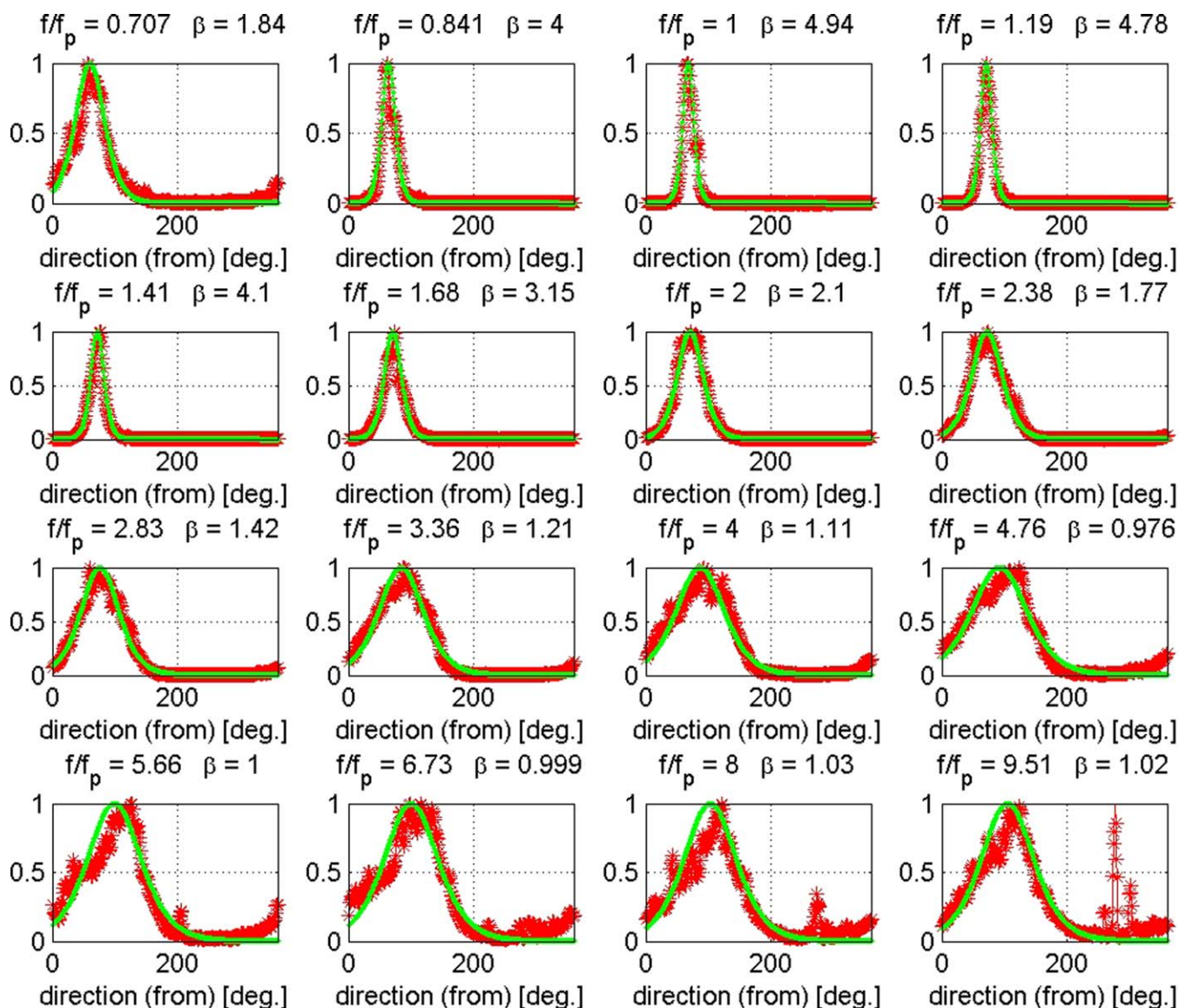


Figure 6. Spreading (run 189—long fetch, strong wind) via WDM. Observed spreading (red); fitted $\text{sech}^2(\beta(\theta - \theta_0))$ (green).

4. Results

4.1. Frequency-Direction Spectra From Wind-Generated Waves

All the methods yield (encounter) frequency-direction spectra $F(f, \theta)$ in polar form such that the variance of surface elevation, σ^2 is given by:

$$\sigma^2 = \int_0^\infty \int_{-\pi}^\pi F(f, \theta) f \, d\theta \, df, \quad (15)$$

where f is the encounter frequency (Hz) and θ is the propagation direction (radians). The spectral densities are in $(\text{m}^2/\text{Hz}^2/\text{radian})$.

A measure of the actual spreading at each frequency may be obtained, via the time series of slopes, from the downwave to crosswave ratio $(\sigma_x/\sigma_y)^2$ of slope variance in each frequency band. (The frequency bands increase in geometrical progression in the WDM analysis. For purposes of comparison, the MLM and MEM estimates, which increase linearly, are summed in the WDM frequency bands.) The spreading is reflected in this downwave to crosswave ratio (DCR) as obtained from the frequency-direction spectra:

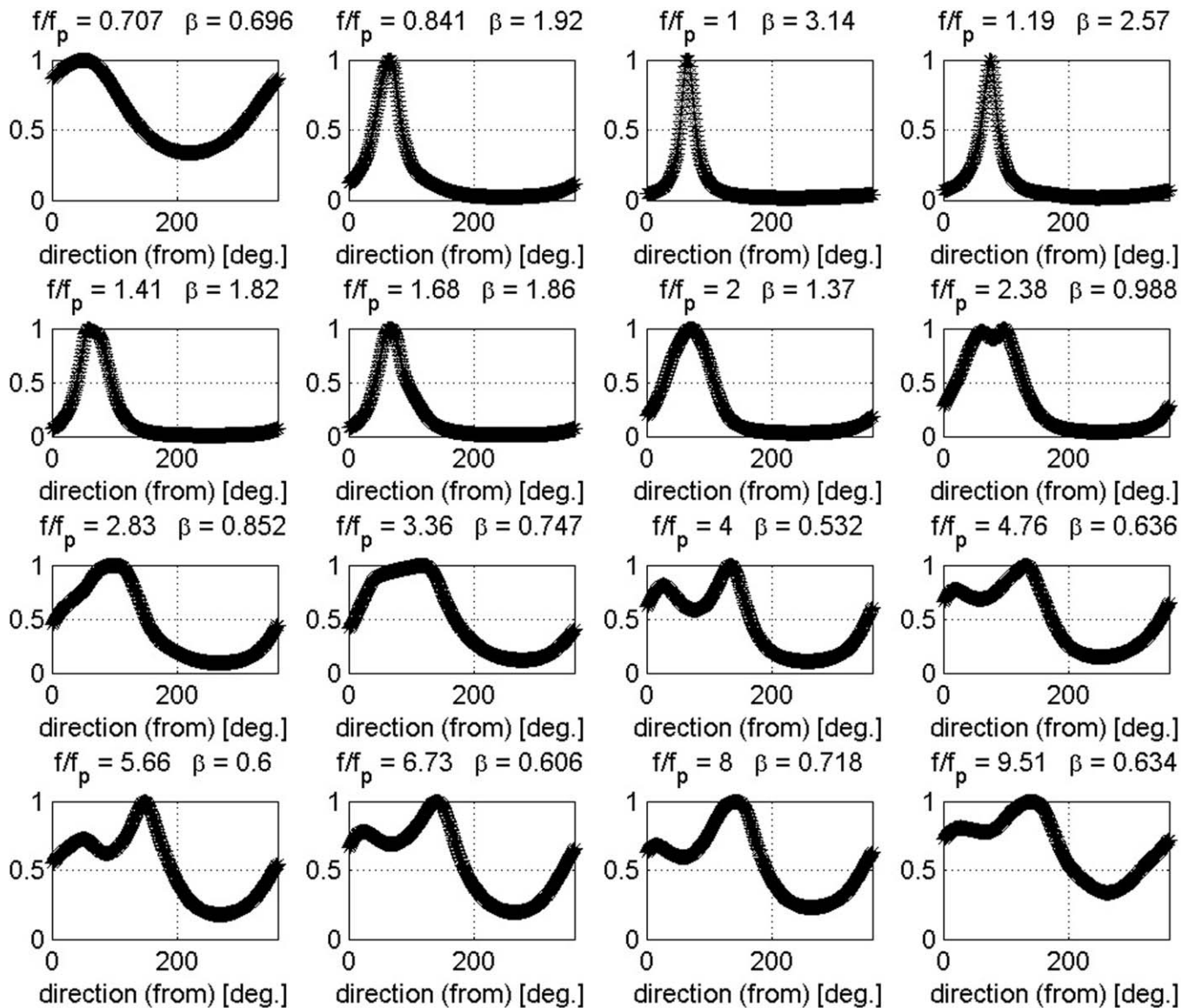


Figure 7. Observed spreading (run 189—long fetch, strong wind) via MLM.

$$DCR(f) = \frac{\int_{-\pi}^{\pi} \cos^2(\theta - \theta_0) D(\theta) d\theta}{\int_{-\pi}^{\pi} \sin^2(\theta - \theta_0) D(\theta) d\theta}, \quad (16)$$

where $D(\theta)$ is the directional energy distribution and θ_0 is the mean wave direction at each frequency. $D(\theta_0) = 1.0$.

The spreading of waves about a mean direction, θ_0 has been modeled by $\text{sech}^2(\beta(\theta - \theta_0))$ [Donelan et al., 1985]. This form is in excellent agreement with the directional distribution determined through WDM—see Figure 1. Unlike the statistical methods (MLM and MEM), WDM reflects the actual distribution of wave energy with direction at the wave array during the time of acquisition of the surface elevation records. Waves occur in groups from various directions. When more than one group (in a given frequency band) from different directions cross the array, WDM reflects energy coming from the bisector direction. This has the effect of narrowing the distribution. On the assumption that the time of coincidence of two or more groups divided by the time of occurrence of a single group is uniform in direction, the WDM observed will be narrower than the actual distribution but unchanged in shape; i.e., the actual distribution will have sech^2 form with a smaller value of β .

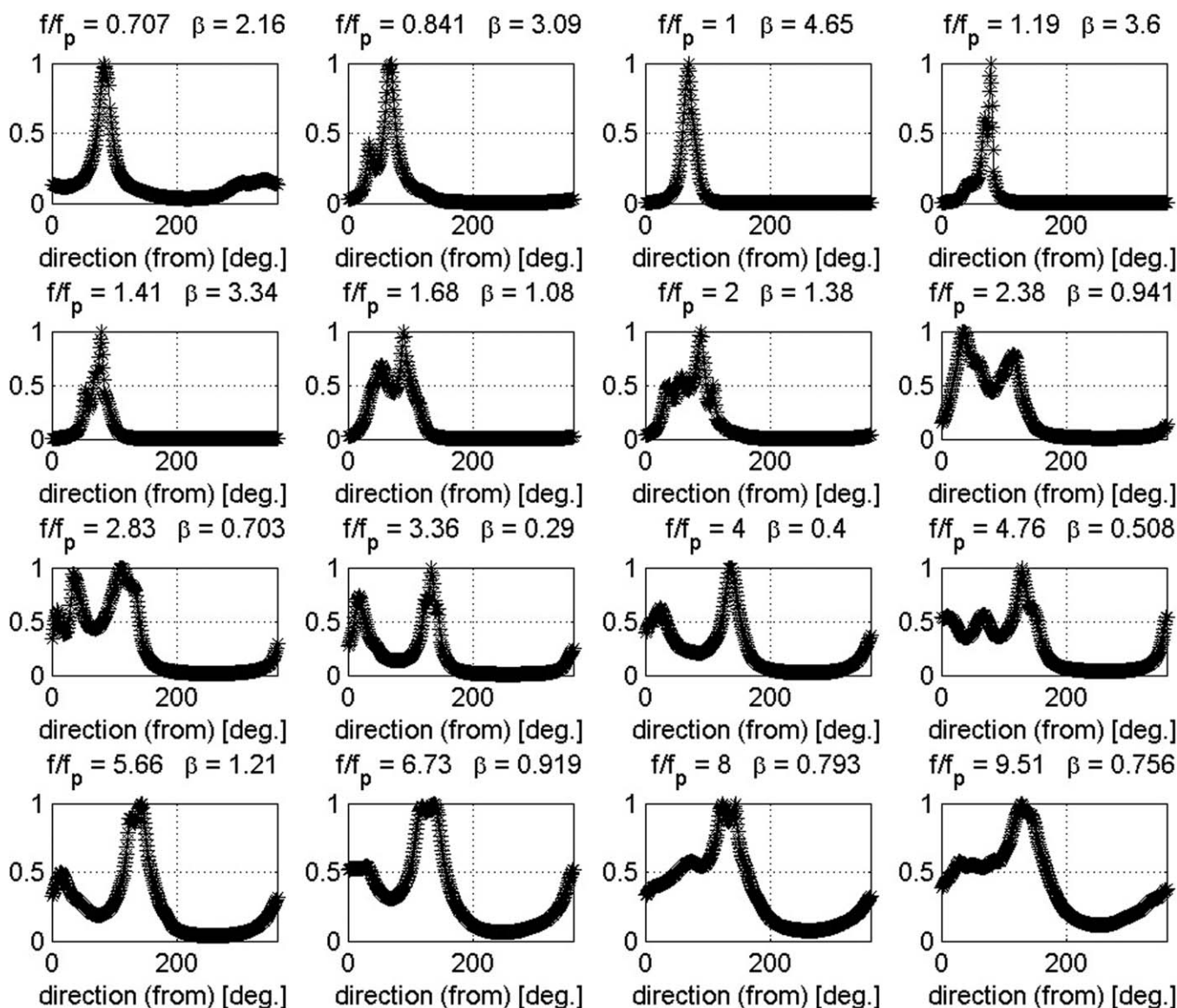


Figure 8. Observed spreading (run 189—long fetch, strong wind) via MEM.

To determine the actual value of β , we note the correspondence between $DCR(f)$ and $\beta(f)$ and report these along with the MLM, MEM, and WDM values in Figure 2. The MLM and MEM directional distributions do not always follow the sech^2 pattern, so we also show the generalized spreading parameter, A defined by [Babanin and Soloviev, 1998]:

$$A^{-1} = \int_{-\pi}^{\pi} D(\theta) d\theta, \quad (17)$$

and

$$A = (\beta/2) \coth(\pi\beta/2). \quad (18)$$

The following tendencies are apparent:

1. WDM is consistently too narrow.
2. MLM is generally too broad.

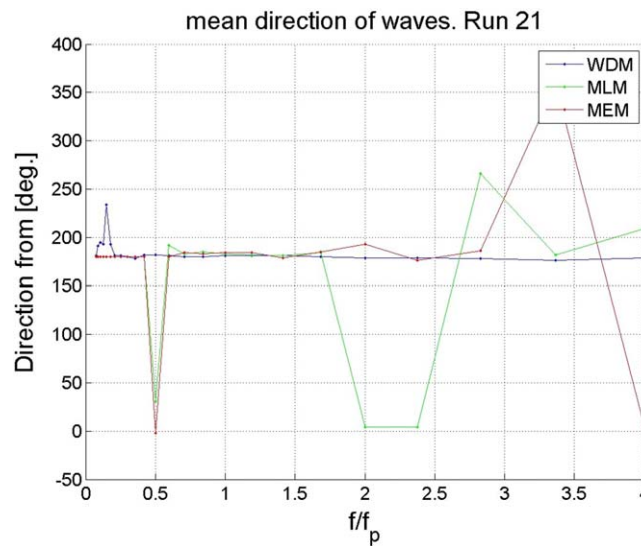


Figure 9. Mean directions (run 21 — $\cos^2\theta$ input spectrum).

the mean direction. The MLM distributions are also unimodal in the well-developed case (run 62), but bimodal above $1.4f_p$ in the strongly forced case (run 82). In both cases, the MLM indicates significant energy at 180° to the mean direction at and above $2f_p$ in the well-developed case, and above $1.2f_p$ in the strongly forced case. The MEM distributions are frequently bimodal but not consistently so; switching between 1 mode and 2 as the frequency increases. Most surprisingly the peak frequency in the strongly forced case (run 82—Figure 4) is strongly and asymmetrically bimodal.

In many applications, the estimate of mean direction is even more important than the directional spread. In Figure 5, we examine the directional estimates from the three methods for a moderately developed case (run 189) with strong winds from the east giving a fetch of about 300 km. f_p is small (0.125 Hz) and the range of f/f_p resolved is large: 0.5 – 13.5. The WDM estimates smoothly vary with advancing frequency, culminating in the wind direction at the shortest waves (55 cm wavelength). The MLM and MEM estimates are noisy and the shortest waves (78 and 55 cm) are 50 and 70 away from the wind direction in the MLM estimates.

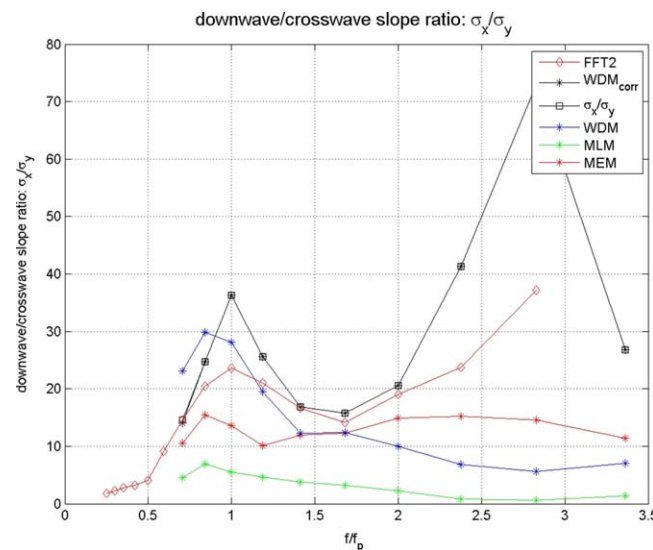


Figure 10. Degree of spreading via downwave/crosswave slope ratio (run 161 — $\cos^{16}\theta$ input spectrum).

3. MEM is far too narrow near the peak and generally too narrow elsewhere.

The corrected WDM spreading distributions are obtained by multiplying the observed distributions by $(\text{sech}^2(\beta_A(\theta-\theta_0))/\text{sech}^2(\beta_0(\theta-\theta_0)))$, where β_0 is the observed value and β_A is the actual value deduced via DCR obtained from the time series of the orthogonal slope components, $\eta_x(t)$ and $\eta_y(t)$. (x is in the θ_0 direction as determined from the WDM analysis). Figures 3 and 4 show the spreads of WDM, MLM, MEM, and the corrected WDM for run 62 (well developed) and run 82 (strongly forced). All the WDM distributions are unimodal and symmetrical about the mean direction with no energy at 180° to

the mean direction. The MLM distributions are also unimodal in the well-developed case (run 62), but bimodal above $1.4f_p$ in the strongly forced case (run 82). In both cases, the MLM indicates significant energy at 180° to the mean direction at and above $2f_p$ in the well-developed case, and above $1.2f_p$ in the strongly forced case. The MEM distributions are frequently bimodal but not consistently so; switching between 1 mode and 2 as the frequency increases. Most surprisingly the peak frequency in the strongly forced case (run 82—Figure 4) is strongly and asymmetrically bimodal.

In many applications, the estimate of mean direction is even more important than the directional spread. In Figure 5, we examine the directional estimates from the three methods for a moderately developed case (run 189) with strong winds from the east giving a fetch of about 300 km. f_p is small (0.125 Hz) and the range of f/f_p resolved is large: 0.5 – 13.5. The WDM estimates smoothly vary with advancing frequency, culminating in the wind direction at the shortest waves (55 cm wavelength). The MLM and MEM estimates are noisy and the shortest waves (78 and 55 cm) are 50 and 70 away from the wind direction in the MLM estimates.

Figures 6, 7, and 8 show the directional spreads for WDM, MLM, and MEM, respectively. The 12 panels cover a wide frequency range from $f/f_p=0.707$ to 9.51 and demonstrate the fidelity of the methods over a wide range (order 10^5) of spectral amplitudes. WDM consistently yields symmetrical unimodal spreads that conform to a $\text{sech}^2(\beta(\theta-\theta_0))$ shape. Whereas MLM and MEM are often bimodal or trimodal and, except near the frequency peak, are not symmetric. Symmetry about the mean direction is expected in a steady wind.

4.2. Frequency-Direction Spectra From Computed-Generated Waves

Cartesian wave number spectra were taken from the model and inverse

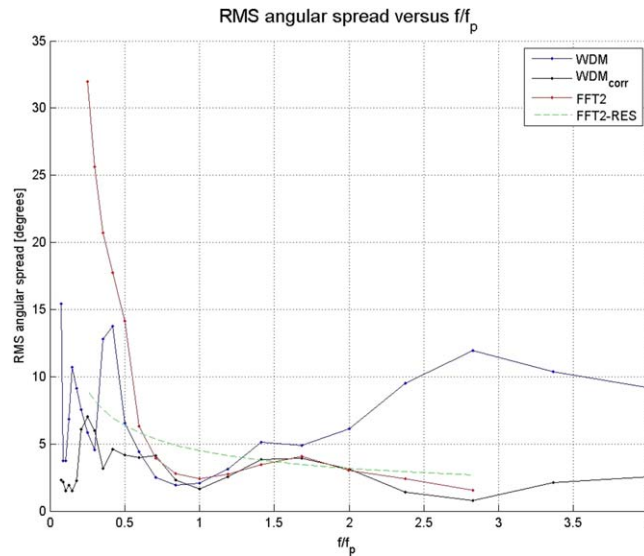


Figure 11. RMS angular spread (run 161 — $\cos^{16}\theta$ input spectrum).

Fourier transformed (IFFT2) to obtain a rectangular array of surface elevations at a given time. 240 of these spectra, separated in time by 4.5 s, were averaged to yield mean wave number spectra. These were then transformed to polar frequency-direction spectra using the theoretical linear dispersion relation. These spectra are labeled FFT2 as they are identical with the spectra that would be obtained from an FFT2 analysis of elevations on the entire grid. The time series, at four points in the center of the array on a square of side 19.5 m, were used to obtain down/crosswave slopes and elevations for input to the WDM, MLM, and MEM methods of estimating frequency-direction spectra.

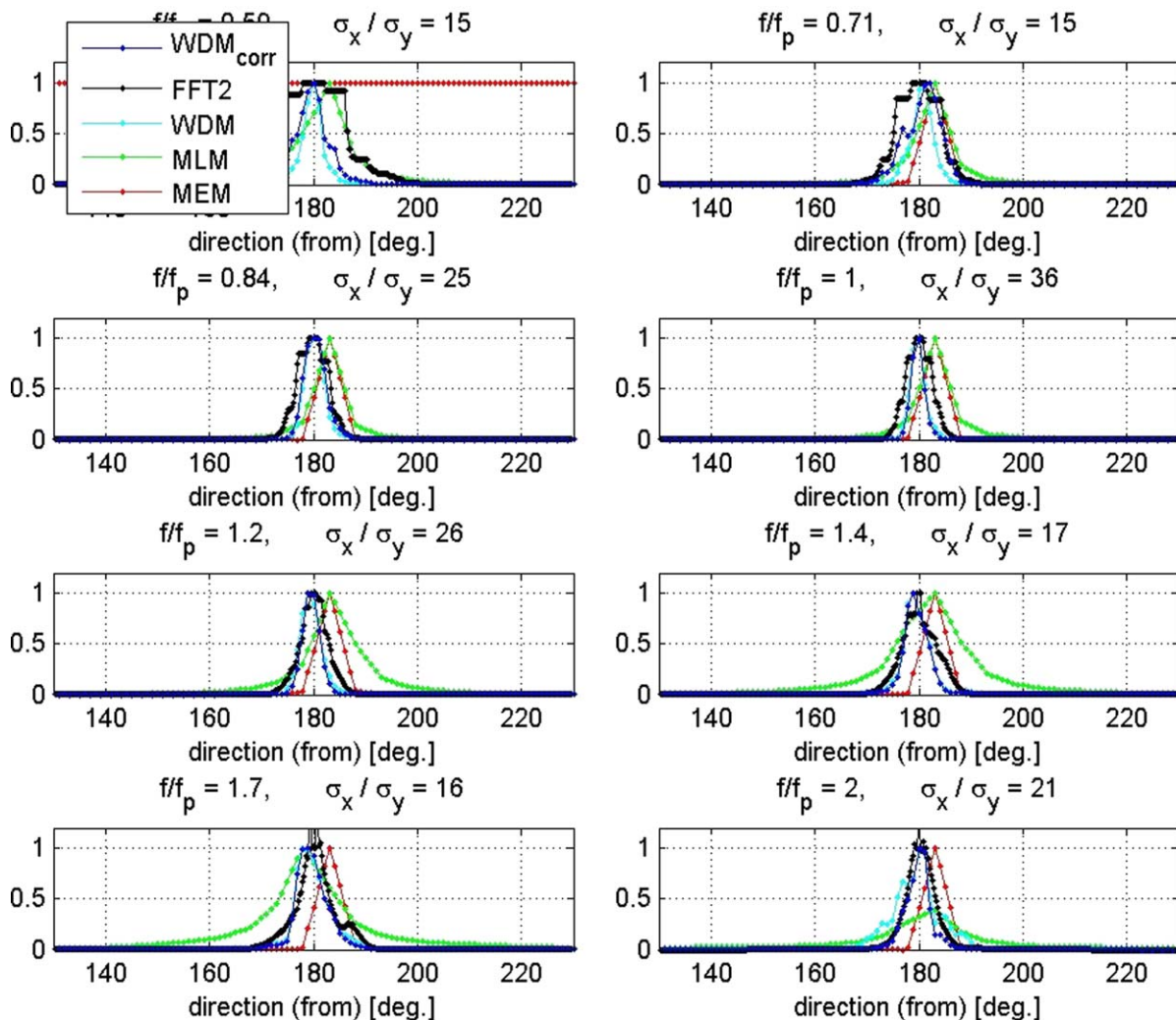


Figure 12. Comparative spreading for run 161 — $\cos^{16}\theta$ input spectrum at various frequencies with respect to the peak.

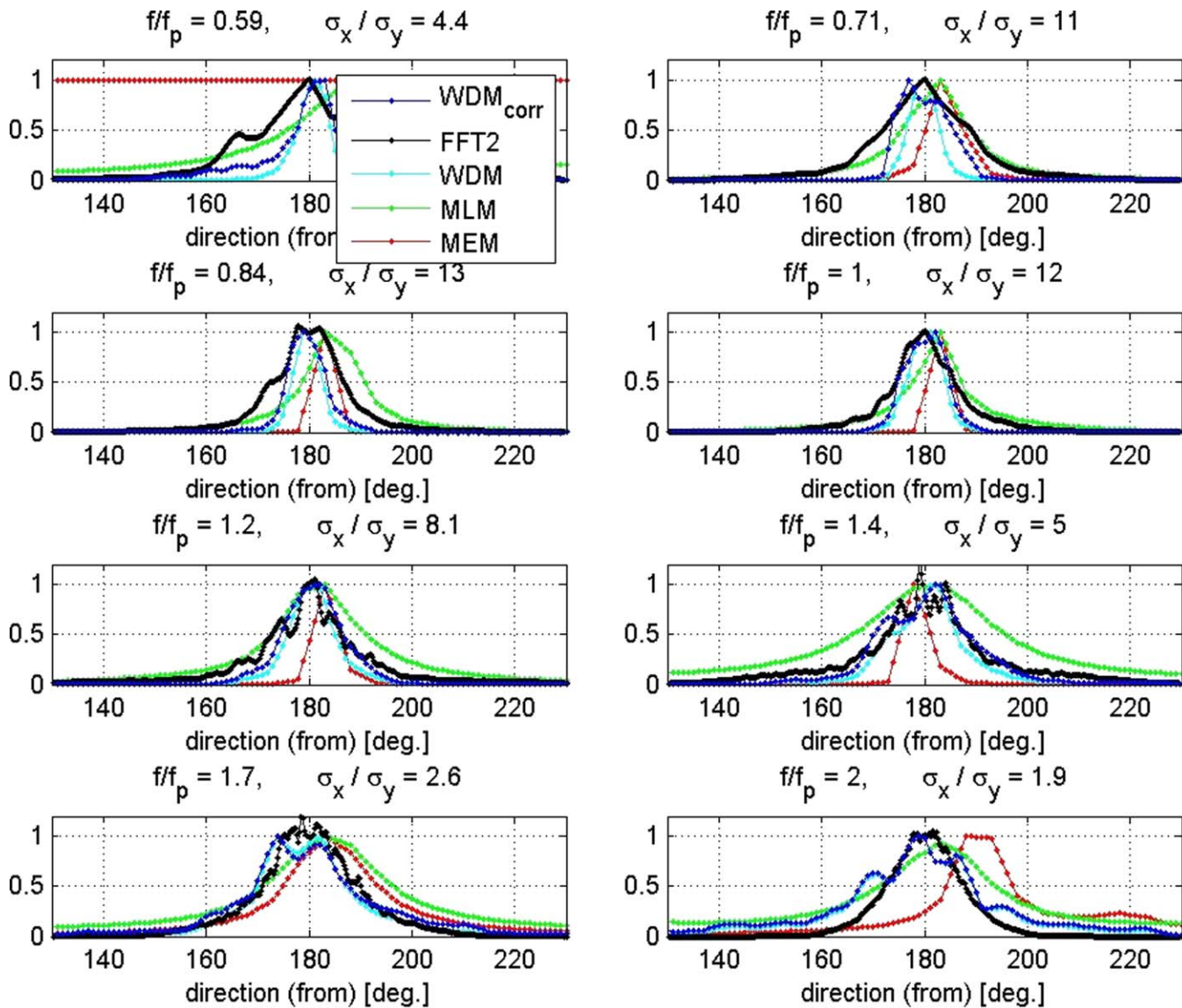


Figure 13. Comparative spreading for run 21 — $\cos^2\theta$ input spectrum at various frequencies with respect to the peak.

The mean directions for the $\cos^2\theta$ input spectrum are shown in Figure 9. Above $0.2f_p$ WDM directions are within a few degrees of downtank (180°); while MLM and MEM are similar in the energy containing region but widely scattered outside of it as in Figure 5 for the field data. In Figure 10, we examine the directional spreading of the narrow ($\cos^{16}\theta$) input spectrum through the ratio of downslope to cross-slope standard deviations, σ_x/σ_y . The actual ratio determined from the time series of slopes (black squares) has a pronounced peak at f_p and another even higher peak at $2.8f_p$. WDM, MEM, and MLM are broader throughout in order of increasing broadness. WDM, having a consistently unimodal shape, is easily adjusted, as described above, to yield WDM_{corr} (black asterisks). The spectra taken from the model wave number spectra (FFT2; red diamonds) are also too broad except between $1.4f_p$ and $2f_p$. This is due to the poor directional resolution of the Cartesian wave number spectra, which is proportional to $f^{-0.5}$ and is compared with the root-mean-square angular spreads of the WDM and FFT2 methods in Figure 11. Here WDM_{corr} , having been adjusted to yield the observed downslope/cross-slope ratio, indicates the actual RMS spreads (black). The resolution of the FFT2 spectra (dashed green line) is adequate only between $1.4f_p$ and $2f_p$, where FFT2 and WDM_{corr} agree. Elsewhere the actual spreads are much smaller than the resolution—leading to broadening of the FFT2 spectra.

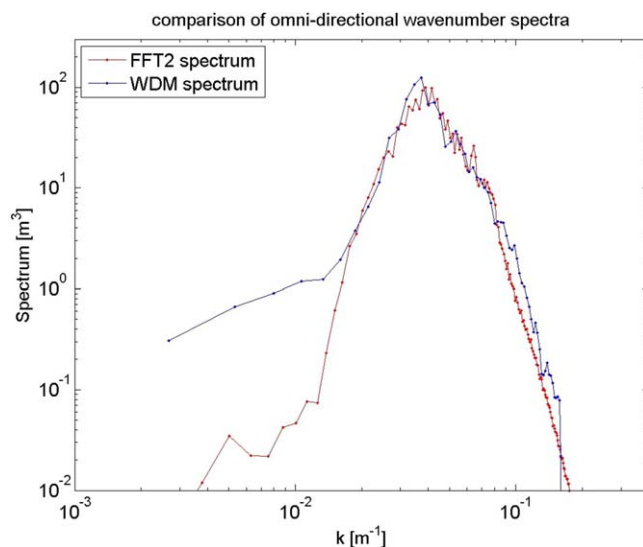


Figure 14. Comparison of wave number spectra from FFT2 and WDM methods (run 161 — $\cos^{16}\theta$).

on axes of wave number and encounter frequency. The peak (0.1 Hz) lies on the linear dispersion curve, while higher frequencies lie between the linear dispersion curve and the dispersion of the second bound harmonics.

5. Summary

The mean directions and directional spreads with frequency are compared for the three methods of estimating frequency-direction spectra: Maximum Likelihood Method (MLM), Maximum Entropy Method (MEM), and Wavelet Directional Method (WDM). Both wind-generated waves and modeled irrotational waves are tested. In the latter case, wave number-direction spectra are obtained through two-dimensional Fourier transforms of the array of modeled surface elevations. The wave number-direction spectra are transformed to frequency-direction spectra using the linear theoretical dispersion relation. These frequency-direction spectra (FFT2), within the directional resolution of the model grid, are a standard against which to compare MLM, MEM, and WDM.

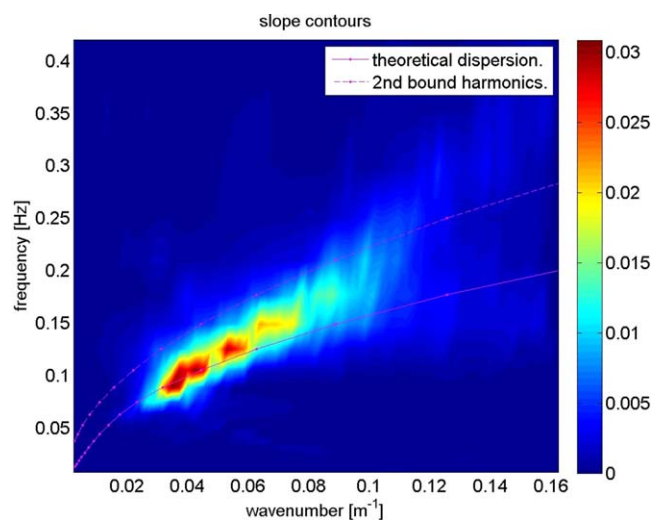


Figure 15. Contours of local slope reveal the dispersion relation via WDM (run 161 — $\cos^{16}\theta$).

All these features—shifting mean directions (MLM, MEM), overbroadening (MLM), underbroadening (MEM), shape similarity (WDM and FFT2), resolution-limited convergence (WDM_{corr} and FFT2)—are illustrated graphically in Figures 12 and 13 for $\cos^{16}\theta$ and $\cos^2\theta$, respectively. The WDM also yields the wave number-directional spectrum. A comparison of the omnidirectional wave number spectrum with FFT2, for the $\cos^{16}\theta$ input spectrum, is shown in Figure 14. The WDM measures wave number, frequency, direction, and amplitude of the waves passing through the array. This allows us to examine various instantaneous and average properties of the wavefield. In Figure 15, the dispersion relation is revealed through contours of RMS slope

The standard methods (MLM and MEM) are too broad (MLM) or too narrow (MEM) and show order 5 degree variability in the peak direction. They are generally unimodal in direction, but are sometimes bimodal (often asymmetric) or trimodal. The frequency-direction spectra of wind-generated seas are consistently unimodal and symmetric about the mean direction [Donelan *et al.*, 1985] and the WDM, which correctly mirrors the spreading shape, reflects this. The WDM is generally a little narrow, but that is easily corrected with the ratio of downslope to cross slope.

The Maximum Likelihood Method and the Maximum Entropy Method require stationarity and yield only the

frequency-direction spectra. The Wavelet Directional Method yields the frequency-direction spectra, wave number-direction spectra, and nonstationary (event) analyses of various wave and group properties. It properly belongs in the toolbox of all wave experimentalists.

Acknowledgments

This work was begun while M.D. was a Visiting Professor in the Centre for Ocean Engineering, Science and Technology. He acknowledges a Visiting Professor grant of Swinburne University, and A.B. acknowledges ONR grant N00014-13-1-0278. The numerical simulations were performed at Swinburne University of Technology's supercomputer facilities "Green machine" and "G2." The wave data used may be obtained by writing to the first author (mdonelan@rsmas.miami.edu).

References

- Babanin, A. V., and Y. P. Soloviev (1998), Variability of directional spectra of wind-generated waves, studied by means of wave staff arrays, *Mar. Freshwater Res.*, *49*, 89–101.
- Borgman, L. (1985), *Maximum-Entropy and Data-Adaptive Procedures in the Investigation of Ocean Waves*, vol. 14, *Fundamental Theories of Physics*, section 21, pp. 429–442, Springer, Dordrecht, Netherlands.
- Capon, J. (1969), High-resolution frequency-wavenumber spectrum analysis, *Proc. IEEE*, *57*(8), 1408–1418.
- Capon, J. (1979), Maximum-likelihood spectral estimation, *Nonlinear Methods Spectral Anal. Top. Appl. Phys.*, *34*, 155–179.
- Chalikov, D., and A. V. Babanin (2013), Three-dimensional periodic fully nonlinear potential waves, paper presented at the ASME 2013 32nd International Conference on Ocean, Offshore and Arctic Engineering, OMAE2013, Am. Soc. of Mech. Eng., Nantes, France.
- Davis, R., and L. Regier (1977), Methods for estimating directional wave spectra from multi-element arrays, *J. Mar. Res.*, *35*(3), 453–478.
- Donelan, M. A., J. Hamilton, and W. H. Hui (1985), Directional spectra of wind-generated waves, *Philos. Trans. R. Soc. London A*, *315*, 509–562.
- Donelan, M. A., W. M. Drennan, and A. K. Magnusson (1996), Non-stationary analysis of the directional properties of propagating waves, *J. Phys. Oceanogr.*, *26*, 1901–1914.
- Farge, M. (1992), Wavelet transforms and their applications to turbulence, *Annu. Rev. Fluid Mech.*, *24*(1), 395–458.
- Hasselmann, K., et al. (1973), *Measurements of Wind-Wave Growth and Swell Decay During the Joint North Sea Wave Project (JONSWAP)*, *Ergänzungsheft zur Deutschen Hydrographischen Zeitschrift Reihe A (8) (Nr. 12)*, 95 pp., Deutsches Hydrographisches Institut, Hamburg, Germany.
- Kaiser, G. (1994), *A Friendly Guide to Wavelets*, Birkhäuser, Boston, Mass.
- Krogstad, H. E. (1988), Maximum likelihood estimation of ocean wave spectra from general arrays of wave gauges, *Model. Identification Control*, *9*(2), 81–97.
- Krogstad, H. E., A. K. Magnusson, and M. A. Donelan (2006), Wavelet and local directional analysis of ocean waves, *Int. J. Offshore Polar Eng.*, *16*(2), 97–103.
- Liu, P. C. (2013), Contemplating ocean wave measurements, *Int. J. Geosci.*, *2013*(4), 229–233, doi:10.4236/ijg.2013.41A019.
- Lygre, A., and H. E. Krogstad (1986), Maximum entropy estimation of the directional distribution in ocean wave spectra, *J. Phys. Oceanogr.*, *16*, 2052–2060.
- Marzetta, T. (1983), A new interpretation of Capon's maximum likelihood method of frequency-wavenumber spectral estimation, *IEEE Trans. Acoust. Speech Signal Process.*, *31*(2), 445–449.
- Nuttall, A. H. (1976), Multivariate linear predictive spectral analysis employing weighted forward and backward averaging: A generalization of Burg's algorithm, report No. TR5501, DTIC Document, Naval Underwater Systems Center, New London, Conn.